J Mol Model (2009) 15:673–679
DOI 10.1007/s00894-009-0464-7

Importance of oligomerisation on *Pseudomonas aeruginosa* Lectin-II binding affinity. *In silico* and *in vitro* mutagenesis

Michaela Wimmerová · Navnit Kumar Mishra · Martina Pokorná · Jaroslav Koča

Received: 9 October 2008 / Accepted: 13 January 2009 / Published online: 11 March 2009

Abstract The effect of terminal GLY114* deletion on the binding affinity of the PA-IIL lectin toward L-fucose was investigated. Both experimental (isothermal titration calorimetry) and computational (molecular dynamics simulations) methods have shown that the deletion mutation decreases the L-fucose affinity. It implies that the PA-IIL saccharide binding affinity is influenced by the dimerization of the lectin. A detailed analysis of computational data confirms the key role of electrostatic interactions in the PA-IIL/saccharide binding.

Keywords Binding free energy · Carbohydrate · Isothermal titration calorimetry · Lectin · Molecular dynamics simulations · Mutagenesis

Abbreviations

PA-IIL	*Pseudomonas aeruginosa* Lectin-II
ITC	Isothermal titration calorimetry
FUC	L-fucose
Me-α-L-Fuc	Methyl-α-L-fucoside
SIE	Solvated interaction energy

M. Wimmerová (✉) · N. K. Mishra · M. Pokorná · J. Koča (✉)
National Centre for Biomolecular Research,
Masaryk University, Faculty Science,
Kotlářská 2, 611 37 Brno, Czech Republic
e-mail: michaw@chemi.muni.cz
e-mail: jkoca@chemi.muni.cz

M. Wimmerová
Department of Biochemistry,
Masaryk University, Faculty of Science,
Kotlářská 2, 611 37 Brno, Czech Republic

Introduction

Protein-carbohydrate interactions play a key role in many biological processes such as immune activity, tumor metastasis, cell-cell interactions, etc. [1, 2]. Proteins responsible for the carbohydrates binding are called lectins and they can be found in all organisms, from viruses, bacteria, plant to mammals [3]. The recognition of host oligosaccharides is also a first step of pathogenic bacteria invasion and infectivity and allows their adhesion to the surface of the host cell. The human opportunistic pathogen *Pseudomonas aeruginosa*, a major cause of morbidity and mortality in cystic fibrosis patients [4], produces high-affinity fucose-binding lectin (PA-IIL) that contributes to the virulence of this pathogenic bacterium [5].

Previous structural and thermodynamical studies have shown that the PA-IIL lectin exhibits high binding affinity to the L-fucose [6, 7]. The acidic pocket of the PA-IIL binding site interacting with the two calcium ions is composed of ASP104, GLU95, ASN103, ASP101, ASP99 and terminal GLY114* from adjacent monomer [8]. This architecture leads to a special requirement for the hydroxyl stereochemistry of the interacting sugar that must be either in $^{1}C_{4}$-L-galacto or $^{4}C_{1}$-D-manno configuration, respectively [7]. Fine specificity of the lectin is derived from other amino acids present in the binding site. *In vitro* site directed mutagenesis has shown the importance of the binding loop in the PA-IIL lectin specificity [9]. Interestingly, terminal GLY114* from the neighboring monomer participates both in calcium coordination and sugar binding through hydrogen bonding.

In the present study, we have focused on one of the issues related to the binding site composed of residues from two different monomers, i.e., if mentioned GLY114* is crucial for the high affinity of the lectin toward mono-

saccharides or it is rather an artificial result of evolution. Importance of the residue for the sugar binding has been studied both experimentally and *in silico*.

We have employed solvated interaction energy [10] and isothermal titration calorimetry [11] for calculation of free energy of binding. The combination of thermodynamic and molecular dynamics simulation data provides not only energy but also the structural information about the binding. We have shown that *in silico* mutagenesis can be one of the tools for the exploration of the ligand affinity and for finding key residues involved in the interaction.

Methods

Isothermal titration calorimetry (ITC) and molecular dynamics (MD) approaches have been applied for the structural-functional characterization of the terminal glycine in the PA-IIL lectin. Deletion mutant was prepared in recombinant form and ITC has been employed to determine thermodynamic parameters of its interaction with sugars. Calculations were performed on the mutant and the wild type lectin to predict the structure and to evaluate binding energy of the protein/sugar complexes.

Experimental methods

Construction of the plasmid for expression of PA-IILΔG114

The oligonucleotides used as primers were as follows: 5′-GGA GAT ACC ATA TGG CAA CAC AAG GAG-3′ (27-mer) and 5′-TTC CAA GCT TCT AGC CGA GCG G-3′ (22-mer). The former introduced NdeI and the latter HindIII restriction sites (underlined sequences), respectively. The latter primer was further designed to remove C-terminal glycine compared with wild-type PA-IIL. PCR was performed using Pfu polymerase (Stratagene Corp, La Jolla, CA) and genomic DNA from *Pseudomonas aeruginosa* ATCC 33347 as a template. After digestion with NdeI and HindIII, the amplified fragment was introduced into multiple cloning sites of pET-25(b+) vector (Novagen, Madison, WI) resulting in plasmid pET25pa2ldG114.

Expression and purification of PA-IIL

E. coli BL21(DE3) cells harboring the plasmid pET25pa2ldG114 were cultured in 1 litre of Luria broth (LB) at 37°C. When the culture reached an optical density of 0.5–0.6 at 600 nm, iso-propyl-β-D-thiogalactopyranoside (IPTG) was added to a final concentration of 0.5 mM. Cells were harvested after 3 h incubation at 30°C, washed and resuspended in 10 ml of the equilibrating buffer (20 mM Tris/HCl, 100 μM $CaCl_2$, pH 7.5). The cells were disrupted by sonication (Soniprep 150, Schoeller instruments, GB). After centrifugation at 10 000 g for 1 h, the supernatant was further purified on Fucose-Agarose (Sigma-Aldrich, USA). PA-IILΔG114 was allowed to bind to the immobilized fucose in the equilibrating buffer and then was eluted by the elution buffer (20 mM Tris/HCl, 100 μM $CaCl_2$, 0.1 M L-fucose, pH 7.5). The purified protein was intensively dialyzed against distilled water for 1 week (for the removal of L-fucose), concentrated by lyophilization and kept at –20°C.

Microcalorimetry

Isothermal titration calorimetry experiments were performed using Microcal VP-ITC microcalorimeter (Microcal, Northampton, MA). All titrations were performed in 0.1 M Tris/HCl buffer containing 3 μM $CaCl_2$, pH 7.5 at 25°C. Aliquots of 10 μl of Me-α-L-Fuc (2 mM) and L-fucose (2.4 mM), respectively, dissolved in the same buffer were added at 5 min intervals to the lectin solution (0.33 mM) present in the calorimeter cell. Three independent titrations were performed for each ligand tested. The temperature of the cell was controlled to 25±0.1°C. Control experiments performed by injections of buffer in the protein solution yielded to insignificant heats of dilution. Integrated heat effects were analysed by non-linear regression using a single site-binding model (Microcal Origin 7). Fitted data yielded the association constant (K_a) and the enthalpy of binding (ΔH). Other thermodynamic parameters, i.e., changes in free energy, ΔG, and entropy, ΔS, were calculated from Eq. (1),

$$\Delta G = \Delta H - T\Delta S = RT \ln K_a \quad (1)$$

where T is the absolute temperature and R=8.314 J.mol^{-1}.K^{-1}.

Computational methods

Construction of PA-IIL/sugar complexes

The starting structure for the wtPA-IIL lectin complexed with L-fucose was taken from the X-ray crystallographic structure (PDB ID: 1UZV, Fig. 1) [8]. The α-methyl-L-fucoside complex was prepared by substitution of hydrogen atom of the anomeric hydroxyl group of L-fucose by the methyl group using Spartan. In the beginning, the bond distance between the O1 and carbon of the added methyl group was 0.9 Å, which after minimization relaxed to the normal bond distance of 1.4 Å. The hydrogen atoms of the protein were added *via* TLEAP of the AMBER.

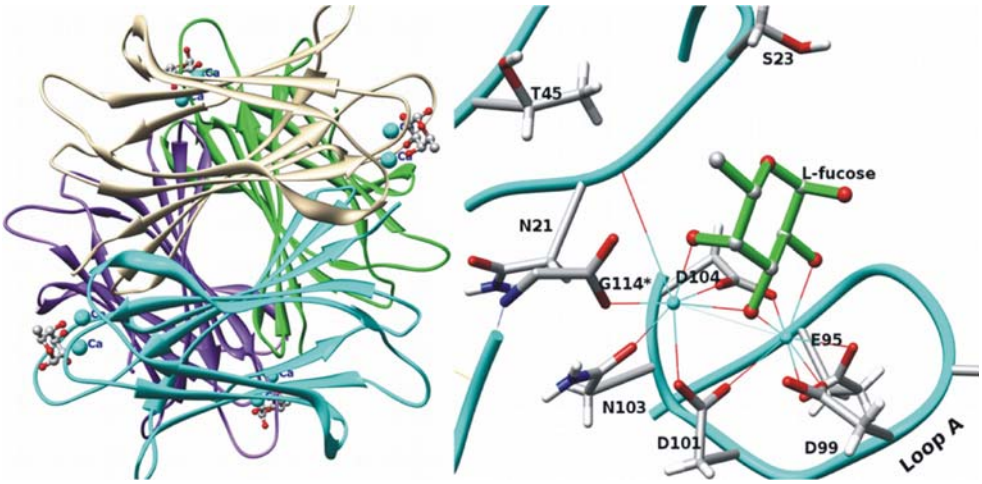

Fig. 1 Crystal structure of tetrameric PA-IIL lectin, each monomer contributes by one binding site. The amino acid residues interacting with L-fucoside *via* two Ca^{2+} ions (cyan spheres) are shown on the right. Graphics prepared using CHIMERA [16] package

Construction of PA-IIL mutant/sugar complexes

The crystal structure has not been refined for the mutant complexes. So, for the calculation, the mutant complexes were prepared by deleting the terminal glycine G114* of the second monomer from the corresponding PA-IIL/sugar complex. The structure of the single point mutants was checked and visualised by the program TRITON developed for *in silico* protein engineering [12].

Molecular dynamics simulations

We have performed molecular dynamics simulations with the wild type lectin (PA-IIL) and its mutant (PA-IILΔG114) in complexes with α-L-fucose and Me-α-L-fucoside. The protein/sugar complexes were prepared using two adjacent monomers from the tetramer crystal structure (Fig. 1) in order to maintain the architecture of the binding site that requires the C-terminus of the adjacent monomer. Previous computational studies have shown that dimeric representation of the PA-IIL/carbohydrate complex reproduces experimental results well [13]. The 10 ns long molecular dynamics simulations were performed for all complexes using the SANDER and PMEMD [14] modules of the AMBER 8 package [15]. The graphics were prepared using CHIMERA [16] package.

The atomic charges for the L-fucose and Me-α-L-fucoside were derived by fitting to HF/6–31G* electrostatic potential (ESP) using the RESP method [17]. The GAFF atom types were defined for both sugars using ANTECHAMBER module of AMBER. The charges and parameters for the protein were taken from the Parm99 force field [17]. Additional force field parameters for the fucose and Me-α-L-fucoside were taken from the GLYCAM04 [18]. The systems were solvated with TIP3P [19] water model forming a truncated octahedral water box. Each calcium ion was described as an ion with two plus charges and van der Waals radius of 1.79 Å [20]. Electrostatic neutrality and isotonic conditions, of the simulated systems were maintained by adding Na^+ and Cl^- ions by using Solvate program [21].

In order to maintain the proper structure, a stepwise equilibration of the system was performed before the free MD simulation. First, the non-crystallographic ions and water molecules were energy minimized. To finish the equilibration of the solvent, a 50 ps long molecular dynamics simulation of ions and water molecules was performed at 298 K. The equilibration continued with energy minimization of the whole system with gradual decreasing of restraints that were imposed on the PA-IIL systems. After the last step, with no restraints on the protein, a 70 ps molecular dynamics with slow heating from 10 K to 298 K was carried out, followed by 30 ps dynamics. Both above MD simulations were carried out under constant pressure of 1 atm. Trajectories were integrated with a 2 fs time step, and the coordinates were saved at each ps. Molecular dynamics simulations were conducted in the NPT ensemble at 298.15 K and 1 atm. The SHAKE algorithm was used to constrain all bond lengths involving hydrogens [22]. The long range electrostatic interactions were treated by the Particle-Mesh Ewald (PME) [23] method with a cut-off of 9 Å. The same cut-off was applied on van der Waals interactions.

Energy analysis for the binding

We have used the SIETRAJ [10] package to calculate free energy from the simulated trajectories. The package calculates the solvated interactions energies (SIE) using five terms and three parameters that have been fitted to reproduce the binding free energies of a data set of 99 ligand protein complexes by Naim et al. [10]. The SIETRAJ is a substitute of MM/PBSA [24] methodology. The SIE calculates the intermolecular Coulomb and van der Waals interaction energies in the bound state, and the

electrostatic contribution for solvation free energy to the binding is the difference of reaction field energy between bound and free states. Reaction field energy is computed by solving Poisson equation with the boundary element method (program BRI BEM [25]). The internal dielectric constant of 2.25 and a solvent dielectric constant of 78.5 were used. The package calculates the free energy ΔG by using the solvated interaction energy formula (Eq. 2).

$$\Delta G = \alpha * \left(E^{c}_{inter} + E^{vdw}_{inter} + \Delta G^{R}_{bind} + \Delta G^{npsol}_{bind} \right) + C \qquad (2)$$

In Equation (2), the E^{c}_{inter} and E^{vdw}_{inter} terms are for the intermolecular Coulomb and van der Waals interaction energies in the bound state, respectively. The electrostatic contribution for solvation free energy ΔG^{R}_{bind} to the binding is the difference of reaction field energy between bound and free states. The ΔG^{npsol}_{bind} term is the solute-solvent van der Waals energy plus the cavitation energy (Eq. 3).

$$\Delta G^{npsol}_{bind} = \gamma * \Delta SA \qquad (3)$$

The cavitation energy is the work done to transfer the solute from vacuum to water and ΔSA is the change in molecular surface area. Scaling cofficient γ of 0.012894 kcal/mol.Å^2 is used for non polar solvation energy calculation, and α of 0.104758 was used for the linear scaling of the couloumb and van der Waals interaction energy and solvation energy. The atomic radii was scaled by a value of rscale=1.1 for the reaction field energy calculation, and a fitting constant C of value -2.89 kcal mol^{-1} was used. The snapshots were taken at the sequential interval of 20 ps to avoid the correlation between two successive conformations.

Results and discussion

Cloning of deletion mutant and production of recombinant PA-IILΔG114 protein in *E. coli*

Using the expression plasmid *pET25pa2ldG114*, the deletion mutant was expressed in *E. coli* BL21(DE3) with a typical yield of about 10 mg of the purified protein per liter of culture. The resulting protein was purified by affinity chromatography on the Fucose-agarose column and run as a sharp band of about 11 kDa on SDS-PAGE. Mass spectrometry analysis confirmed the molecular mass of 11.674 kDa, corresponding to the PA-IILΔG114 amino acid sequence lacking the initial methionine residue.

Structure-functional characterization of PA-IILΔG114

In order to evaluate importance of the C-terminal glycine for the binding affinity, the protein was crystallized in a presence of Me-α-Fuc and its thermodynamic parameters of binding were determined using ITC. The PA-IILΔG114 mutant crystallized in presence of ammonium sulfate in P212121 space group. Data were collected at ESRF

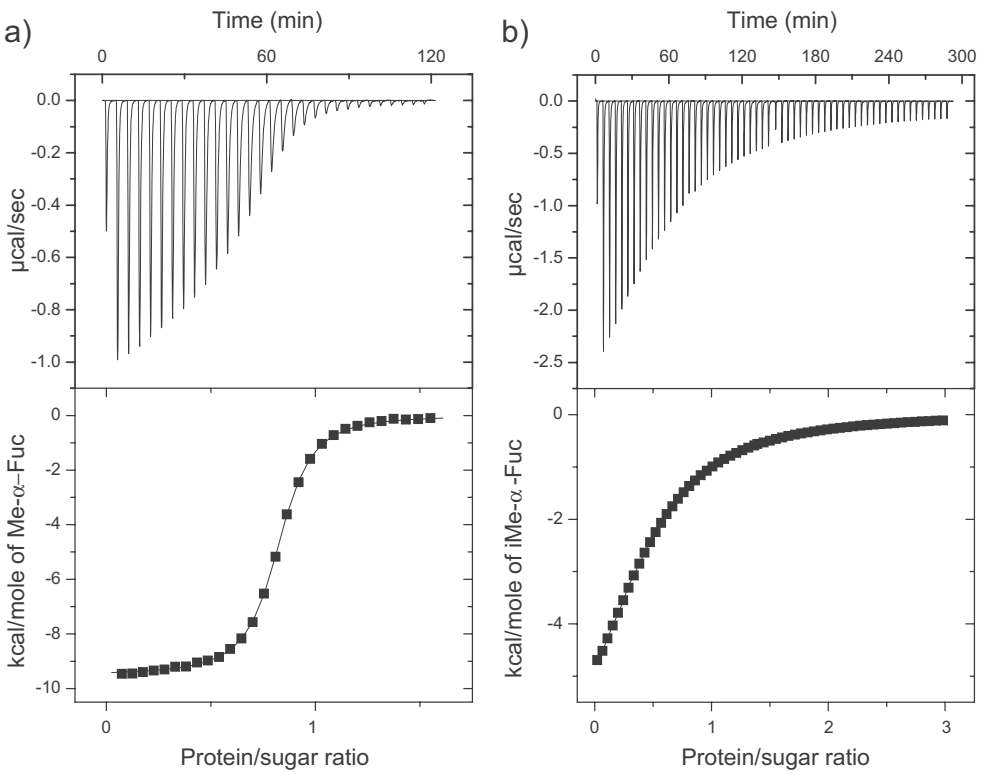

Fig. 2 A) Titration microcalorimetry results of Me-α-Fuc (2 mM) binding to PA-IILΔG114 (0.33 mM) in 0.1 M Tris buffer, pH 7.5 with 30 µM $CaCl_2$. Top: data obtained from 60 automatic injections (10 µl) of Me-α-Fuc each into the lectin-containing cell. Bottom: plot of the total heat released as a function of total ligand concentration for the titration shown in the upper panel. The solid line represents the best least-squares fit for the obtained data. B) Titration microcalorimetry data for PA-IIL interaction with Me-α-fuc (adapted from [7])

Table 1 Thermodynamics of binding for wild type PA-IIL and PA-IILΔG114 with L-fucose and Me-α-Fuc by ITC at 293 K (standard deviations were calculated from three independent measurements for both ligands)

[a] taken from [6]

[b] taken from [7]

	$K_A \times 10^4$ (M^{-1})	$K_D \times 10^{-6}$ (M)	ΔG (kJmol^{-1})	ΔH (kJmol^{-1})	-TΔS (kJmol^{-1})
L-Fuc					
PA-IIL [a]	12.0 (±1.0)	8.3 (±0.7)	-29.0 (±0.1)	-27.7 (±0.5)	-1.3 (±0.5)
PA-IILΔG114	0.24 (±0.002)	434 (±2.8)	-19.2 (±0.1)	-24.2 (±0.3)	5.0 (±0.3)
Me-α-L-Fuc					
PA-IIL [b]	235 (±8)	0.43 (±0.01)	-36.4 (±0.1)	-41.3 (±1)	4.9 (±1)
PA-IILΔG114	1.2 (±0.2)	82 (±18)	-23.3 (±0.5)	-33.0 (±0.3)	9.6 (±0.2)

beamline ID14–2 at 1.4 Å resolution. Structure was solved by molecular replacement using native PA-IIL structure (PDB code 1GZT) but it was not further refined since no electron density of the ligand was observed in the binding sites and binding loops of the protein were disordered.

Thermodynamic data were recorded for the interaction of PA-IIL and its mutant with L-fucose and α-methyl-L-fucoside, respectively, as the best monosaccharides for PA-IIL. The use of a methyl derivative of the sugar also avoids the problems related to anomeric disorder in solution and moreover gives a better mimic of real biological interactions. The comparison of ITC results for PA-IIL and PA-IILΔG114 mutant interactions with α-methyl-L-fucoside is shown in Fig. 2. As expected, the results exhibited a monotonic decrease in the exothermic heat of the binding until saturation was achieved. Decrease in affinity of binding of the mutated protein is directly visible from the changed heat profile. Precise values of equilibrium association constant Ka, binding enthalpy ΔH, and stoichiometry of interaction per monomer n were obtained by fitting the classical equation for single-site binding [11]. The other thermodynamic parameters, free energy and entropy of binding (ΔG and ΔS), were calculated as described in the Methods. The thermodynamic data of the interaction of PA-IIL and its mutant with both sugars is summarized in Table 1. The comparison of data obtained with the deletion mutant with results obtained for wild-type PA-IIL indicates that both lectins bind preferentially to the methyl derivative of fucose, as commonly observed in protein-carbohydrate interactions, but deletion of the terminal glycine leads to decrease in affinity by two orders of magnitude.

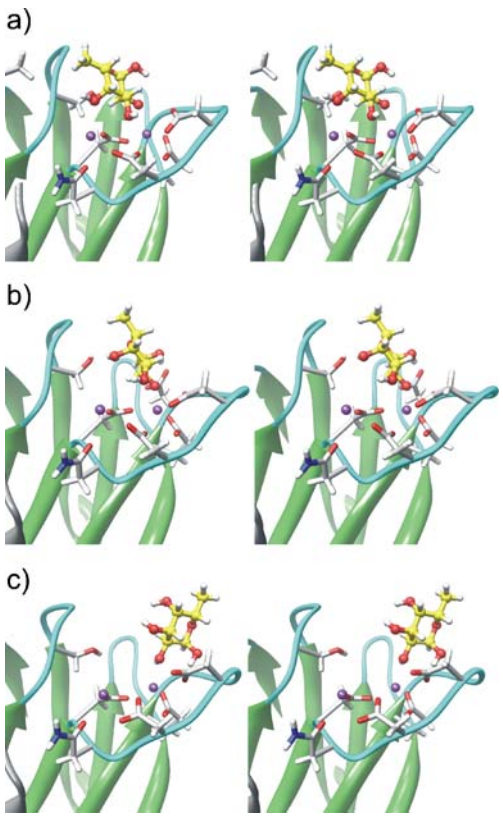

Fig. 3 Stereo view snapshots from the PA-IILΔG114/FUC MD simulation. (a) In the initial snapshot, the l-fucose is coordinated with both calcium ions, (b) the snapshot at is coordinated with both calcium ions, (b) the snapshot at 5th ns shows coordination of O2 and O3 with CAL-II. (**c**) In the snapshot at 9.8th ns, L-fucose shows further rotation inside the binding site, but still keeps coordination with one of the two calcium ions. Graphics prepared using CHIMERA [16] package

Analysis of molecular dynamics trajectories

To quantify stability of the trajectories, RMSDs from initial x-ray structure was calculated (not shown here). There was no large conformational drift in the PA-IIL trajectory. There

Table 2 ΔG for interaction of PA-IIL and its mutant with α-L-fucose

	Interaction energy (kJmol^{-1})		Solvation energy (kJmol^{-1})		ΔG (kJmol^{-1})
	E^c_{inter}	E^{vdw}_{inter}	ΔG^R_{bind}	ΔG^{npsol}_{bind}	
L-Fuc					
PA-IIL	-182.8	-14.4	100.9	-11.2	-23.4 (1.2)
PA-IILΔG114	-141.2	-15.7	104.3	-9.4	-18.6 (2.4)
Me-α-L-Fuc					
PA-IIL	-195.8	-10.8	112.8	-11.8	-23.2 (1.5)
PA-IILΔG114	-191.6	-16.3	126.5	-10.8	-21.8 (1.1)

The E^c_{inter} and the E^{vdw}_{inter} terms are for the intermolecular Coulomb and van der Waals interaction energies in the bound state, respectively. ΔG^R_{bind} is the electrostatic contribution to the solvation free energy, which is the difference of reaction field energy between bound and free states. The ΔG^{npsol}_{bind} of the binding is the solute-solvent van der Waals energy plus the cavitation energy

is only initial 1.2 Å rise for the C alpha RMSDs in the beginning of the trajectory and then the RMSDs becomes stable. However, the situation is somewhat different for the PA-IILΔG114 trajectory, which shows a drift at 2.5 ns and becomes stable. This drift confirms that the binding site of the mutant must be somewhat reorganized.

In the PA-IIL/FUC trajectory, the O2, O3, and O4 of the L-fucose are always coordinated with at least one Ca^{2+} ion. The O3 and O4 are coordinated with the Ca^{2+} ion, which is proximal to the glycine of the second monomer (for this study assigned as CAL-I), the O2 and O3 are coordinated with the second Ca^{2+} ion (assigned as CAL-II). In contrary, during the PA-IILΔG114/FUC simulation, the ligand has moved to adopt substantially different position (Fig. 3). From the beginning of the trajectory till about three ns, the sugar is in similar configuration and exhibits the same coordination as in the wild type PA-IIL. From 5 ns to 9 ns, the O2 and O3 of the L-fucose remain coordinated with CAL-II while O4 lost the coordination with CAL-I. During the last 1 ns, the sugar becomes coordinated with CAL-II by O2. The deletion of glycine allows for entering of some water molecules close to the CAL-I to fulfill the coordination sphere of the ion. This was confirmed by radial distribution function, which was separately calculated for the oxygen atoms from the monosaccharide, protein, and water distribution around the calcium ion (not shown here).

The calculated binding free energy for the L-fucose to the mutant lectin is lower compared to the wild type lectin (Table 2). The electrostatic interaction energy is less favorable by -9.08 kcal mol^{-1} for the mutant. The presence of water around the O4 of the L-fucose in PA-IILΔG114 increases the polar solvation energy by about 1 kcal mol^{-1}. The absence of terminal glycine decreases the electrostatic contribution for the binding. The CAL-I is fixed on its position by water molecules. The desolvation energy associated with the binding of L-fucose/α-methyl-L-fucoside for the mutated PA-IIL is higher than those for the PA-IIL lectin. Because the desolvation energy represents enthalpy in the calculation, it would imply entropy increasing for the mutant/carbohydrate binding. It corresponds to experimental entropies (Table 1). It is seen that also simulation data for Me-α-L-fucoside confirms our conclusions about importance of terminal glycine. However, the calculated free energy is not in such a good agreement with experiment as it is for L-fucose itself. The reason is probably related to the sampling problem as FUC trajectories started with the X-ray structure while only the "homology modeling" obtained structure was used for Me-α-L-fuc. One cannot exclude also an influence of the parameters for the free energy calculation, which can be better for non-methylated monosaccharides compared to methylated ones. Anyway, all the results suggest that the terminal glycine of the second monomer has a significant role in carbohydrate binding.

Conclusions

In the present work we have shown the importance of the terminal glycine from adjacent monomer in the PA-IIL lectin affinity. The deletion of the terminal glycine residue results in affinity decrease by two orders of magnitude. The calculated decomposition of binding free energy clearly shows that the key role of the GLY114 of the adjacent monomer for the interaction is played by its electrostatic contribution. The paper also shows that *in silico* mutagenesis can be used as a useful tool that complements experiments and brings detailed information about protein/carbohydrate binding in terms of both structure and energy.

Acknowledgments This work was funded by the Ministry of Education (MSM0021622413 to M.P., LC06030 to J.K., ME08008 to M.W.) of the Czech Republic.

References

1. Rudd PM, Elliott T, Cresswell P, Wilson IA, Dwek RA (2001) Glycosylation and the immune system. Science 291:2370–2376
2. Scanlan CN, Offer J, Zitzmann N, Dwek RA (2007) Exploiting the defensive sugars of HIV-1 for drug and vaccine design. Nature 446:1038–1045
3. Dam TK, Brewer CF (2002) Thermodynamic studies of lectin-carbohydrate interactions by isothermal titration calorimetry. Chem Rev 102:387–430
4. Roussel P, Lamblin G (2003) The glycosylation of airway mucins in cystic fibrosis and its relationship with lung infection by Pseudomonas aeruginosa. Adv Exp Med Biol 535:17–32
5. Gilboa-Garber N (1982) *Pseudomonas aeruginosa* lectins. Methods Enzymol 83:378–385
6. Perret S, Sabin C, Dumon C, Pokorná M, Gautier C, Galanina O, Ilia S, Bovin N, Nicaise M, Desmadril M, Gilboa-Garber N, Wimmerová M, Mitchell EP, Imberty A (2005) Structural basis for the interaction between human milk oligosaccharides and the bacterial lectin PA-IIL of *Pseudomonas aeruginosa*. Biochem J 389:325–332
7. Sabin C, Mitchell EP, Pokorna M, Gautier C, Utille JP, Wimmerova M, Imberty A (2006) Binding of different monosaccharides by lectin PA-IIL from *Pseudomonas aeruginosa*: thermodynamics data correlated with X-ray structures. FEBS Lett 580:982–987
8. Mitchell EP, Sabin S, Snajdrova L, Pokorna M, Perret S, Gautier C, Hofr C, Gilboa-Garber N, Koca J, Wimmerova M, Imberty A (2005) High affinity fucose binding of *Pseudomonas aeruginosa* lectin PA-IIL: 1.0 A resolution crystal structure of the complex combined with thermodynamics and computational chemistry approaches. Proteins: Struct Funct Bioinf 58:735–748
9. Adam J, Pokorna M, Sabin C, Mitchell E, Imberty A, Wimmerova M (2007) Engineering of PA-IIL lectin from *Pseudomonas aeruginosa* - Unravelling the role of the specificity loop for sugar preference. BMC Struct Biol 7:36
10. Naim M, Bhat S, Rankin KN, Dennis S, Chowdhury SF, Siddiqi I, Drabik P, Sulea T, Bayly CI, Jakalian A, Purisima EO (2007) Solvated interaction energy (SIE) for scoring protein-ligand binding affinities. 1. Exploring the parameter space. J Chem Inf Model 47:122–133
11. Wiseman T, Williston S, Brandts JF, Lung-Nan L (1989) Rapid measurement of binding constants and heats of binding using a new titration calorimeter. Anal Biochem 179:131–137

12. Prokop M, Adam J, Kriz Z, Wimmerova M, Koca J (2008) TRITON: a graphical tool for ligand-binding protein engineering. Bioinformatics 24:1955–1956
13. Mishra NK, Kulhánek P, Snajdrová L, Petrek P, Imberty A, Koca J (2008) Molecular dynamics study of *Pseudomonas aeruginosa* lectin-II complexed with monosaccharides. Proteins: Struct Funct Bioinf 72:382–392
14. Robert ED, Pedersen LG (2003) PMEMD 3, University of North Carolina-Chapel Hill. PMEMD 3, University of North Carolina-Chapel Hill
15. Case DA, Darden TA, Cheatham III TE, Simmerling CL, Wang J, Duke RE, Luo R, Merz KM, Wang B, Pearlman DA, Crowley M, Brozell S, Tsui V, Gohlke H, Mongan J, Hornak V, Cui G, Beroza P, Schafmeister C, Caldwell JW, Ross WS, Kollman PA (2004) AMBER 8, 2004,. AMBER 8, University of California, San Francisco
16. Pettersen EF, Goddard TD, Huang CC, Couch GS, Greenblatt DM, Meng EC, Ferrin TE (2004) UCSF Chimera - A visualization system for exploratory research and analysis. J Comp Chem 25:1605–1612
17. Wang J, Cieplak P, Kollman PA (2000) How well does a restrained electrostatic potential (RESP) model perform in calculating conformational energies of organic and biological molecules? J Comput Chem 21:1049–1074
18. Kirschner KN, Woods RJ (2001) Solvent interactions determine carbohydrate conformation. Proc Natl Acad Sci USA 98:10541–10545
19. Jorgensen WL, Chandrasekhar J, Madura JD, Impey RW, Klein ML (1983) Comparison of simple potential functions for simulating liquid water. J Chem Phys 79:926–935
20. Bradbrook GM, Gleichmann T, Harrop SJ, Habash J, Raftery J, Kalb (Gilboa) J, Yariv J, Hillier IH, Helliwell JR (1989) X-Ray and molecular dynamics studies of concanavalin-A glucoside and mannoside complexes Relating structure to thermodynamics of binding. J Chem Soc Faraday Trans 94:1603–1611
21. Grumbmuller H (1996) Solvate: a program to create atomic solvent models. Electronic access: www.mpibpc.gwdg.de/abteilungen/071/hgrub/solvate/docu.html
22. Ryckaert JP, Ciccotti G, Berendsen HJC (1977) Numerical integration of the cartesian equations of motion of a system with constraints: molecular dynamics of n-alkanes. J Comp Phys 23:327–341
23. Darden T, York D, Pedersen L (1993) Particle mesh Ewald: An N [center-dot] log(N) method for Ewald sums in large systems. J Chem Phys 98:10089–10092
24. Kollman PA, Massova I, Reyes C, Kuhn B, Huo S, Chong L, Lee M, Lee T, Duan Y, Wang W, Donini O, Cieplak P, Srinivasan J, Case DA, Cheatham TE III (2000) Calculating structures and free energies of complex molecules: Combining molecular mechanics and continuum models. Acc Chem Res 33:889–897
25. Purisima EO (1998) Fast summation boundary element method for calculating solvation free energies of macromolecules. J Comp Chem 19:1494–1504